

Photoemission studies and electronic structure of U_2T_2In (T = Ni, Rh, Pt) compounds

This article has been downloaded from IOPscience. Please scroll down to see the full text article.

2006 J. Phys.: Condens. Matter 18 4355

(<http://iopscience.iop.org/0953-8984/18/17/021>)

View [the table of contents for this issue](#), or go to the [journal homepage](#) for more

Download details:

IP Address: 129.252.86.83

The article was downloaded on 28/05/2010 at 10:25

Please note that [terms and conditions apply](#).

Photoemission studies and electronic structure of U_2T_2In ($T = Ni, Rh, Pt$) compounds

A Szytuła^{1,5}, A Jezierski², A Winiarski³, B Penc¹ and V H Tran⁴

¹ M Smoluchowski Institute of Physics, Jagiellonian University, Reymonta 4, 30-059 Kraków, Poland

² Institute of Molecular Physics, Polish Academy of Sciences, Smoluchowskiego 17, 60-179 Poznań, Poland

³ A Chełkowski Institute of Physics, University of Silesia, Uniwersytecka 4, 40-007 Katowice, Poland

⁴ W Trzebiatowski Institute of Low Temperature and Structure Research, Polish Academy of Sciences, 50-950 Wrocław, PO Box 937, Poland

E-mail: szytula@if.uj.edu.pl

Received 2 January 2006

Published 13 April 2006

Online at stacks.iop.org/JPhysCM/18/4355

Abstract

The electronic structure of the tetragonal U_2T_2In ($T = Ni, Rh, Pt$) compounds in the paramagnetic phase were studied by x-ray photoelectron spectroscopy (XPS). Both valence band and core level spectra were analysed. The experimental data are compared with the calculations of the density of states using the tight-binding linear muffin-tin orbital method (TB-LMTO) and full-potential local-orbital full-relativistic method (FPLO). The calculated data reveal a dominant U 5f electron character for the states near the Fermi level E_F with a small contribution from U 5d, Ni 3d, Rh 4d, Pt 5d and In 5p states. The XPS valence bands of these compounds are characterized by a sharp peak of the U 5f states near the Fermi level (E_F) and broad peaks of the Ni 3d, Rh 4d and Pt 5d states at about 2.6, 3.2 and 4.0 eV below E_F , respectively. The small change in the position of the U 5f peak with respect to E_F is -0.35 eV for $T = Ni$ and -0.15 eV for $T = Rh$ and Pt . A satellite between the Ni $2p_{1/2}$ and Ni $2p_{3/2}$ peaks is visible, suggesting that the Ni 3d band is not completely filled, and the existence of a small induced magnetic moment on the Ni atoms cannot be ruled out.

1. Introduction

Uranium intermetallic compounds, especially those containing a transition d-electron metal (T) and a p-electron element (X), form an interesting class of materials. During the last decade

⁵ Author to whom any correspondence should be addressed.

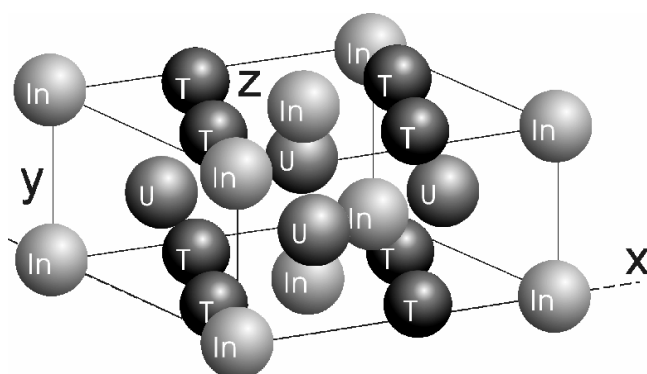


Figure 1. Crystal unit cell of U_2T_2In ($T = Ni, Rh, Pt$) compounds.

these intermetallics have attracted a particular interest because of their anomalous behaviour observed at low temperatures. Among these uranium compounds there is a new group of uranium ternary intermetallics having the common chemical formula U_2T_2X , for which the physical properties have widely been investigated both experimentally and theoretically [1–18]. The majority of these compounds crystallize in the tetragonal U_3Si_2 -type structure (space group $P4/mbm$, $Z = 2$) [1, 2]. The crystal unit cell is presented in figure 1. The U atoms occupy the 4h positions, whereas the In and T atoms are located at the 2a and 4g positions, respectively. This structure is a layer structure that consists of two kinds of layers stacked along the c -axis with the interval of $c/2$. The uranium atoms occupy solely one basal plane, whereas T and In atoms share the other one (see figure 1). U_2Pt_2In and few others adopt a superstructure of the Zr_3Al_2 -type ($P4_2/mnm$, $Z = 4$), that doubles the unit cell in the c -direction and shifts the atoms slightly from their symmetric positions. In contrast to compounds of the U_3Si_2 -type, uranium atoms in U_2Pt_2In are placed in two inequivalent sites [13].

The experimental works [1–18] have indicated that the 2:2:1 intermetallics exhibit a large variety of electronic and magnetic properties, also including exotic phenomena such as spin-fluctuation (U_2Rh_2In [5, 11]), Kondo insulator (U_2Ru_2Sn [17]) and heavy-fermion (U_2Pt_2In [18]) phenomena. Some of the compounds order antiferromagnetically at low temperatures, often displaying a complex magnetic structure [7–9, 13]. It is assumed that these interesting properties are due to hybridization of the 5f electrons of the uranium atom with the electrons of the ligands [10].

The U_2T_2In compounds ($T = Ni, Rh$ and Pt) investigated in this work exhibit diverse magnetic behaviours [5].

- Antiferromagnetic ordering is observed for $T = Ni$ with the Néel temperature 14.3 K. Neutron diffraction measurements indicated that the uranium atoms carry magnetic moments of $0.58 \mu_B$ [8], $0.85 \mu_B$ [9] or $0.92 \mu_B$ [13], respectively. All the values are considerably reduced in comparison to the theoretical moment of the free U^{3+} ion ($3.27 \mu_B$).
- The magnetic susceptibility $\chi(T)$ of U_2Rh_2In obeys the Curie–Weiss law above 120 K. At low temperatures it exhibits a broad peak with a maximum at $T = 6$ K [11].
- U_2Pt_2In exhibits a large increase in magnetic susceptibility $\chi(T)$ when cooled down to 1.6 K and is classified as a spin fluctuation system with a nonmagnetic ground state [5]. The single crystal susceptibility data reveal a weak maximum at 7.9 K which indicates the presence of a short-range correlation [18].

An enhancement in the electronic specific heat has furthermore been observed at low temperatures (200, 280 and 850 mJ/mol f.u. K^2 for U_2Ni_2In , U_2Rh_2In and U_2Pt_2In , respectively [6]). In addition, the specific heat curve of U_2Pt_2In develops a temperature dependence $C_p/T \sim \ln T$, appropriate to a non-Fermi liquid (NFL) state. Furthermore, the electrical resistivity data of this compound have supported the NFL behaviour [18]. Basically, the resistivity of U_2Rh_2In varies with temperatures above 10 K in similar manner as U_2Pt_2In does, i.e., typical of compounds showing spin fluctuation phenomenon, like UA_2 and UPt_3 . For U_2Ni_2In , the $\rho(T)$ data revealed a broad temperature region of negative slope, probably associated with the Kondo effect.

In the case of U_2Rh_2In and U_2Pt_2In , the absence of any clear anomaly in the temperature dependence of the specific heat in the temperature range 2–300 K indicates that they are paramagnetic. We are convinced that the difference in the properties of the studied compounds originates from a difference in the electronic structure, which is influenced by subtle 5f-electron–ligand hybridization. The U–U distances in all three reported compounds [3, 13] are slightly above the Hill limit (~ 3.5 Å) for uranium compounds [19], so the direct exchange between the uranium magnetic ions is no longer the dominating factor for the magnetic properties. Instead, an analysis of the data suggests that there exists a competition between the RKKY interaction and the Kondo effect, which provides these compounds to adopt a Doniach phase diagram [10].

In order to gain new information about the electronic structure of these compounds we have performed x-ray photoelectron spectroscopy (XPS) measurements and tight-binding linear muffin-tin orbital (TB-LMTO) calculations in the atomic spheres approximation (ASA) [20] and full-potential local-orbital full-relativistic with the spin–orbit coupling (FPLO) [21, 22] band-structure calculations. We hope that a comparison between theoretical predictions and experimental data allows to draw conclusions about the electronic structure, in particular the electronic state of uranium atoms.

Previously, electronic structure calculations within the frame of the LCAO method have been carried out for U_2T_2In ($T = Co, Ni, Pd$) [4, 5, 23], U_2T_2Sn ($T = Co, Rh, Ir, Ni, Pd, Pt$) [24] and U_2T_2Sn ($T = Fe, Co, Ni$) [25]. The result of these calculations was to indicate that the electronic structure and related properties of U_2T_2In compounds mainly originate from the interplay between the band filling of transition-metal d-states and hybridization between the d-states of the T atoms and f-states of the U atoms.

2. Experimental details

2.1. Sample preparation and purity check

The samples studied in this study, with a total amount of about 1 g each, were prepared by arc-melting of the stoichiometric amounts of the constituent elements (purity 99.8% for U, 99.999% for Ni, Pt, Rh and 99.9999% for In) on a water-cooled copper hearth using a non-consumable throated tungsten electrode in a protective Ti-gettered high-purity argon atmosphere. After melting, the weight loss was negligible (less than 0.5% weight). For the purpose of homogenization, as-cast samples were wrapped in Ta foil, sealed in an evacuated silica tube and annealed at 650 °C for two weeks. The phase composition was checked by powder x-ray diffraction (XRD) employing Cu $K\alpha$ radiation. The chemical composition was determined with an energy-dispersive x-ray (EDX) spectrometer PV9800. The x-ray examination showed that the compounds are single phase and crystallize in the tetragonal U_3Si_2 -type structure for U_2T_2In ($T = Ni, Rh$) and Zr_3Al_2 -type for U_2Pt_2In . The calculated lattice parameters, $a = 7.381(3)$ Å and $c = 3.581(2)$ Å for U_2Ni_2In , $a = 7.554(4)$ Å and $c = 3.605(2)$ Å for U_2Rh_2In and $a = 7.672(6)$ Å and $c = 7.483(7)$ Å for U_2Pt_2In , do not

differ from those published earlier [10–12], and the amount of impurity phases does not exceed 2% weight.

2.2. Electronic structure measurements

The XPS spectra in a broad range of binding energy (0–1300 eV) were recorded at room temperature in a PHI 5700/660 Physical Electronics photoelectron spectrometer using a monochromatized Al $K\alpha$ x-ray source ($h\nu = 1486.6$ eV). All measurements were performed under ultra-high vacuum (UHV) conditions in the region of 10^{-10} Torr. The energy spectra of the electrons were analysed by a hemispherical mirror analyser with an energy resolution of ~ 0.3 eV. The Fermi level was referred to the gold Au $4f_{7/2}$ binding energy at -84.0 eV. The spectrometer was calibrated using Au $4f_{7/2}$ (-84.0 eV), Ag $3d_{5/2}$ (-368.1 eV) and Cu $2p_{3/2}$ (932.5 eV). The emission spectra were collected after mechanical cleaning of the sample in the preparation chamber under UHV conditions (1×10^{-9} Torr) and then the sample was introduced into the spectrometer (5×10^{-10} Torr). Each spectrum was measured immediately after breaking the sample in vacuum. Uranium compounds are chemically active and sample surfaces are degraded owing to oxidation [26, 27]. The oxidation of the sample was checked by observing the O 1s spectra before and after each measurement. The C 1s peak is also observed in the investigated spectra.

3. Electronic structure calculation

The tight-binding linear muffin-tin orbital (TB-LMTO) method in the atomic spheres approximation (ASA) [20] and FPLO (full-potential local orbital—full relativistic with the spin orbit coupling) method [21, 22] were used to compute the electronic density of states (DOS) of U_2T_2In ($T = Ni, Rh, Pt$). In the LMTO method we applied the scalar-relativistic approximation for the band electron and a fully relativistic treatment for the frozen core electron. In the ASA the values of the atomic spheres radii were taken in such a way that the sum of all the atomic sphere volumes was equal to the volume of the unit cell. The compounds with $T = Ni$ and Rh have the tetragonal structure (U_3Si_2 -type with the space group $P4/mbm$) and the unit cell contains two formula units with $N = 10$ atoms each [1, 2]. The input for the computations is the tetragonal unit cell as provided in [1, 2], and experimental values of the lattice constants and position parameters were taken from these references. The calculations were performed for the paramagnetic and ferromagnetic phases. In the LMTO calculations the atomic configurations were assumed according to the periodic table of elements and for uranium atom we included the 6p electrons into the valence band. The exchange–correlation potential was assumed to be in the form of von Barth and Hedin [28] and nonlocal corrections were also used [29]. The self-consistent spin-polarized band calculations were carried out for 405 k -points in the irreducible wedge of the Brillouin zone. For U_2Pt_2In we have also calculated the electronic density of states (DOS) for the Zr_3Al_2 -type structure (space group $P4_2/mnm$ ($Z = 4$)) [13]. This structure corresponds to doubling of the unit cell in the c -direction. The lattice parameters and the positions of atoms were taken from [13]. The electronic densities of states were calculated for the paramagnetic and ferromagnetic phases.

In order to study the effect of spin–orbit coupling on the electronic density of states we used the full-potential local-orbit method (FPLO-5) [21, 22, 30] in the full relativistic version with spin–orbit coupling. The calculations were carried out for the U_2T_2In ($T = Ni, Rh, Pt$) system for a tetragonal structure with 10 atoms per unit cell for U_2T_2In ($T = Ni, Rh$) and 20 atoms per unit cell for U_2Pt_2In . For the calculations we assumed the following configurations of atoms: U core + semi core ($6s6p$) + $5f^36d^17s^2$ (6 valence electrons), Ni: core + $3d^84s^2$ (10 valence

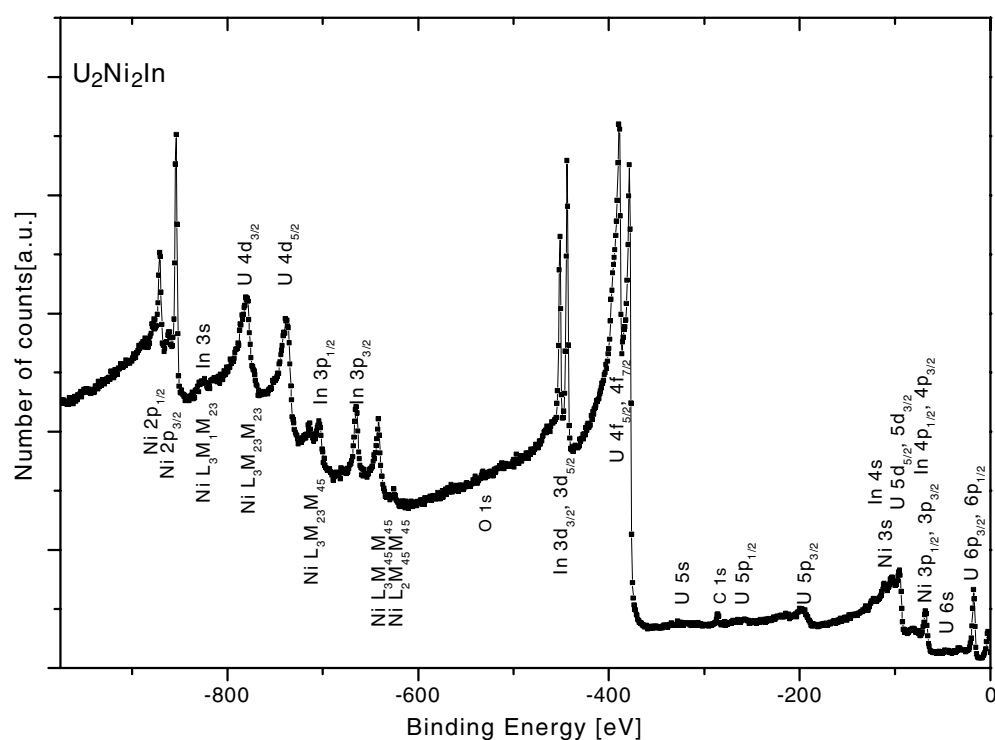


Figure 2. XPS Al $K\alpha$ spectrum of the U_2Ni_2In compound (with the core level lines) in the wide binding energy range of 0–970 eV.

electrons), Rh: core + $4d^85s^1$ (9 valence electrons), Pt: core + $5d^96s^1$ (10 valence electrons), In: core + $5s^25p^14d^{10}$ (13 valence electrons). In this way in the U_2T_2In ($T = Ni, Rh, Pt$) system we included in the calculations for 45, 43 and 45 valence electrons, respectively (table 2). The calculations were performed for the reciprocal space mesh containing 196 points within the irreducible wedge of the Brillouin zone. The exchange–correlation potential was assumed in the form proposed by Perdew and Wang [31]. The densities of states were calculated for the paramagnetic and ferromagnetic phases.

The theoretical photoemission spectra were obtained from the calculated density of states (DOS) convoluted by a Lorentzian with a half-width equal to 0.4 eV and scaled using the proper photoelectronic cross sections for partial states [32].

4. Results

As an example, the XPS spectrum for U_2Ni_2In in the energy range 0–970 eV is shown in figure 2. Besides the peaks corresponding to the U, Ni and In elements, small intensity peaks are found at -283.5 eV for C 1s and at -531.0 eV for O 1s. A similar situation is observed for the two other compounds.

The results of the quantitative analysis of the investigated spectra (in atomic%) are given in table 1. They indicate a small concentration of oxygen and a larger one of carbon. The carbon is probably connected with the low purity of uranium (99.8%). The peak corresponding to O 1s has two components with binding energies 530 and 532 eV. The first line probably corresponds to uranium oxides (UO_2 —530.4 eV or UO_3 —529.9 eV) and the second to the residue gas.

Table 1. Atomic concentration (in percentage) determined from the XPS spectra for U_2T_2In ($T = Ni, R, Pt$).

Compounds	U	In	T	C 1s	O 1s
U_2Ni_2In	34.74	19.26	35.01	9.66	1.32
U_2Rh_2In	30.35	15.84	31.89	18.68	3.25
U_2Pt_2In	32.32	16.76	33.18	15.29	2.45

Table 2. The difference between the total energy of ferromagnetic and paramagnetic phase $\Delta E = E(\text{ferro}) - E(\text{para})$ in U_2T_2In ($T = Ni, Rh, Pt$) (tetragonal) compounds calculated by LMTO and FPLO methods. The last result denotes the value for the doubled unit cell.

	ΔE (Ryd) (LMTO)	ΔE (Ryd) (FPLO)
U_2Ni_2In (tet)	-3.9063	
U_2Rh_2In (tet)	+4.9795	+0.0187
U_2Pt_2In (tet)	-5.0969	+0.0040
U_2Pt_2In (doubled)	-9.8199	

4.1. Valence band

The XPS valence bands of all three U_2T_2In ($T = Ni, Rh, Pt$) compounds are shown in figure 3. These experimental data can be directly compared with the calculated paramagnetic density of states (DOS) by TB-LMTO-ASA and FPLO methods (figures 4 and 5). In figure 4 we present the total and partial DOS for the particular atoms: U, T (Ni, Rh, Pt) and In, respectively. By inspecting figure 4 we can see that the occupied part of the DOS can be decomposed into two regions. The first region, near to the Fermi level, consists of the 5f, 6d and 7s states of the uranium atoms and the states of the Ni (3d+4s), Rh (4d+5s), Pt (5d+6s) and In (5s+5p) atoms. The second narrow band, with the maximum at -19.0 eV, corresponds to the U $6p_{3/2}$, In $4d_{5/2}$ and In $4d_{3/2}$ electrons. In the scalar-relativistic LMTO calculation we do not observe the splitting of the 5f uranium peak near the Fermi energy.

Figure 5 shows the calculated total density of states obtained from the full-relativistic FPLO method. The full-potential scalar-relativistic FPLO calculations (not visualized here) showed that the total density of states had a similar shape as the DOS obtained by the LMTO method. The main difference between the LMTO and full-relativistic FPLO calculations is visualized in the splitting of 5f states of uranium (near the Fermi level) and 6p states of U and 4d states of In. The two peaks corresponding to In $4d_{5/2}$ and In $4d_{3/2}$ are at -13.6 and -14.5 eV while the peak corresponding to U $6p_{3/2}$ is at -17.1 eV. The positions of these peaks show large shifts in comparison to the tabulated data for pure elements (-16.6 and -17.4 eV for In $4d_{5/2}$ and In $4d_{3/2}$ and -16.9 eV for U $6p_{3/2}$ [33]); however, they seem to be independent of the T element.

Both methods (scalar-relativistic LMTO and full-relativistic FPLO) give similar shapes of the densities of states.

- The unoccupied part of the DOS above the Fermi level E_F consists of the 5f electrons from U with a signature of spin-orbit splitting (in FPLO). The splitting is not observed in scalar-relativistic LMTO.
- A broad peak with the maximum at -2.6 eV for U_2Ni_2In would correspond to Ni 3d, at -3.2 eV for U_2Rh_2In to Rh 4d and at -4.0 eV for U_2Pt_2In to Pt 5d states.
- The 4s states for the Ni, 5s states for Rh and 6s for Pt, and 7s-electrons of the uranium atoms form a broad maximum below and above the Fermi level.
- 6d states of uranium form a broad peak with the maximum at -4.4 eV.

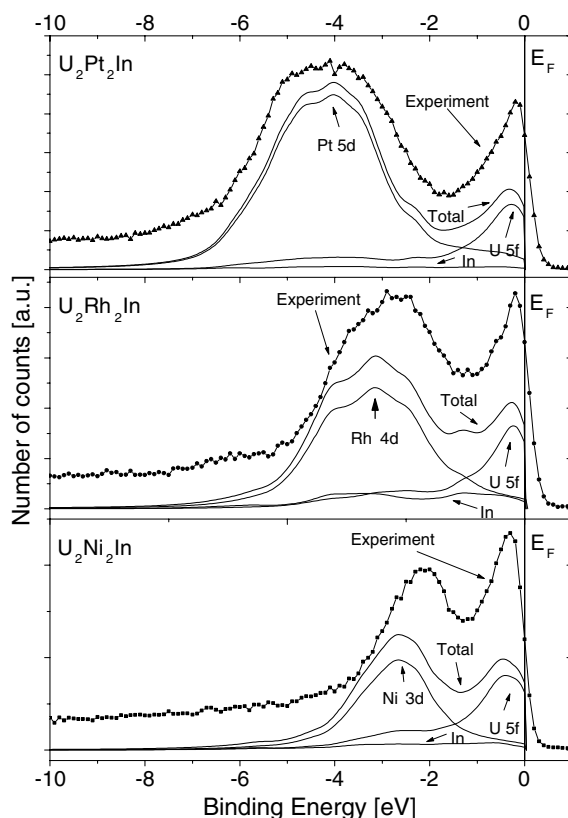


Figure 3. Comparison of the measured (square points) and calculated (light lines for individual components and thick line for total) XPS spectra of valence bands for paramagnetic U_2T_2In ($T = Ni, Rh, Pt$) compounds. The total density of states convolved with Lorentzians of FWHM 0.4 eV taking into account proper photoelectronic cross sections from [32] for bands with different symmetry give the calculated XPS spectra. The Fermi level E_F level located at $E = 0$ eV is marked by the vertical solid line.

- In 5s states form a narrow band at -5.6 eV for U_2Ni_2In , -5.8 eV for U_2Rh_2In and -6.3 eV for U_2Pt_2In , respectively,
- In 5p states form a broad band below and above the Fermi level.

We have also calculated the electronic density of states for the spin-polarized systems. For U_2Ni_2In and U_2Pt_2In the total energies of the system obtained in LMTO and FPLO for the ferromagnetic phase were higher than for the paramagnetic systems. We calculated the difference $\Delta E = E(\text{ferro}) - E(\text{para})$ for all the systems, and the results are listed in table 2. The spin-polarized LMTO calculations gave the following values of the magnetic moment of uranium: 1.9, 2.1 and 2.41 μ_B for $T = Ni, Rh, Pt$; however, from FPLO we have obtained for uranium the spin (orbital) magnetic moments as follows: 0.37 (-0.79) μ_B for $T = Rh$ and 1.1 (-1.69) μ_B for $T = Pt$.

The spin-polarized LMTO calculation for the tetragonal structures indicates that the ferromagnetic phase in U_2Rh_2In is more stable than the paramagnetic phase; however, FPLO calculation has shown that the difference between the paramagnetic and ferromagnetic phase in U_2Rh_2In and U_2Pt_2In is small.

In the case of the U_2Pt_2In system we performed the LMTO band calculation for the structure with the space group $P4_2/mnm$ (doubled unit cell (20 atoms)) with the atom positions

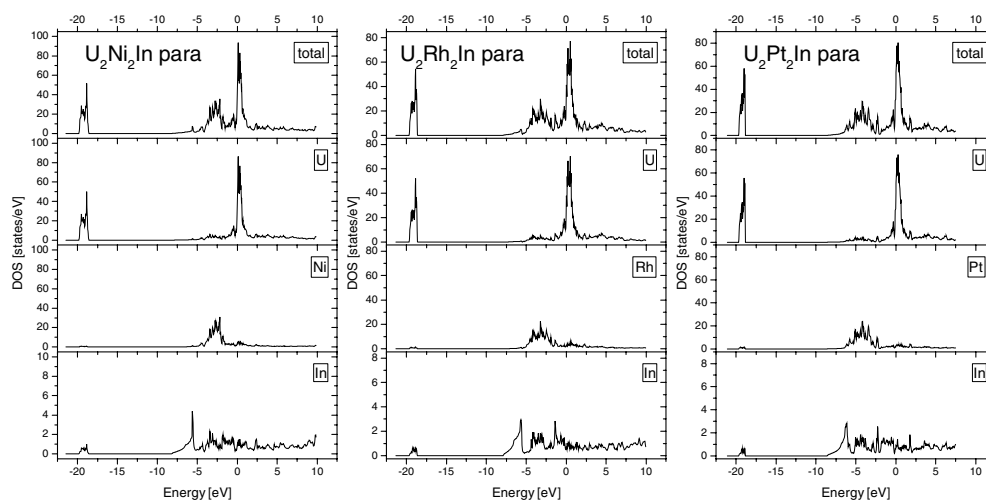


Figure 4. The total density of states and the contribution from U, T elements (Ni, Rh, Pt) and In to the total density of states of paramagnetic U_2T_2In ($T = Ni, Rh, Pt$) compounds calculated by the TB-LMTO method. The Fermi level is located at $E = 0$ eV.

according to [13]. The total energy analysis shows that the system is paramagnetic at 0 K. The shape of the total density of states is similar to that obtained for the U_2T_2In ($T = Ni, Rh$) series of compounds (figure 4).

All experimental spectra (see figure 3) are characterized by two peaks near E_F . The first one lies below the Fermi level at -0.35 eV for U_2Ni_2In and -0.15 eV for U_2Rh_2In and U_2Pt_2In . These rather sharp peaks would correspond to the U 5f states. The second one, located below E_F , is somewhat broad, at -2.0 eV corresponding to the Ni 3d states in U_2Ni_2In , -2.7 eV for Rh 4d states in U_2Rh_2In and -4.0 eV for Pt 5d states in U_2Pt_2In . The widths of these peaks are found to amount to 2.1 eV in U_2Ni_2In , 2.6 eV in U_2Rh_2In and 3.3 eV in U_2Pt_2In .

The experimental data are compared with the calculated XPS spectra. The calculated shapes of the peaks reproduce the experimental ones. The data corresponding to the positions of the U 5f and Pt 5d states agree, while those for Ni 3d and Rh 4d are shifted by 0.7 eV towards the low-energy side.

The In 5s and In 5p states form a broad maximum with small intensities.

4.2. Core levels

4.2.1. Uranium core levels. The XPS spectra of U $4f_{7/2}$ and U $4f_{5/2}$ core electronic states are shown in figure 6. The U 4f spectrum is analysed based on two asymmetric lines resulting from $4f_{7/2}$ and $4f_{5/2}$ with strong intensities and two weak asymmetric satellites with binding energies about 1 eV and about 7 eV higher than the main line. In the analysis of these spectra it is necessary to take into account the influence of the uranium oxides, which causes an increase in the intensities in the region of the binding energy at -380.0 and -390.5 eV.

The complex structure of the uranium 4f states, besides screening effects, is caused by multiplet splitting due to exchange interactions between the 4f hole and the 5f electrons ($j-j$ coupling) after the photoemission process. Such a multiplet splitting for rare earth 4d and 5p exists in the form of a widespread structure [34–36]. Each line of U 4f, which due to spin–orbit coupling splits into U $4f_{7/2}$ and U $4f_{5/2}$, may be additionally split due to the coupling of the hole 4f states ($l = 3; s = \pm 1/2; j = 7/2, 5/2$) with the 5f states. The

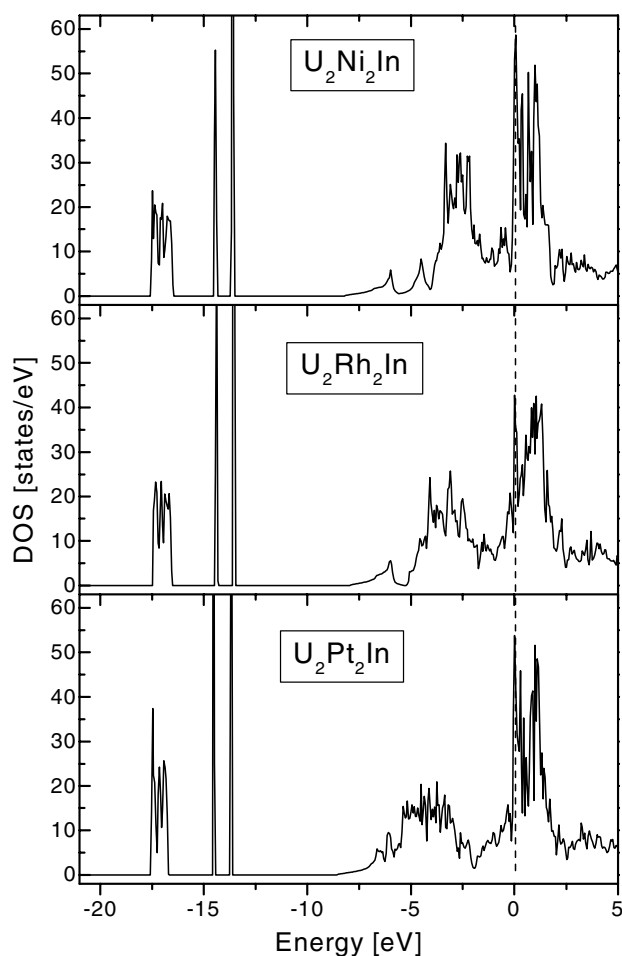


Figure 5. The total density states of paramagnetic U_2T_2In ($T = Ni, Rh, Pt$) compounds calculated by the FPLO method. The vertical broken line shows the position of the Fermi energy E_F .

structure of the 4f lines, consisting of the main line and two satellites, can be interpreted as a result of different contributions of the $5f^2$, $5f^3$ and $5f^4$ final states in the photoemission processes. This interpretation is consistent with the so-called dualism of the 5f electrons that has recently been considered much in intermetallic uranium compounds [37–39]. The physical origin of the asymmetry of the main lines of the XPS spectra was described by the screening of the 4f core-hole potential by the 5f electrons on the neighboring U atoms [40, 41]. The complex spectra can be decomposed according to the Doniach–Sunjić theory [42], after subtracting the background using the Tougaard method [43]. For U_2Ni_2In the main line is split due to spin–orbit coupling into two lines at the binding energies -377.1 eV ($U 4f_{7/2}$) and -387.9 eV ($U 4f_{5/2}$). These values are in good agreement with the reference values -377.2 and -388.2 eV, respectively [33] as observed in other uranium compounds [44–48]. Each of these lines consists of dominant asymmetric lines with a singularity index α of about 0.41 and two symmetric satellites at positions -378.5 and -384.7 eV. A similar spectrum is observed for U_2Rh_2In and U_2Pt_2In . The parameters characterizing the XPS spectra of U_2Ni_2In , U_2Rh_2In and U_2Pt_2In are collected in table 3.

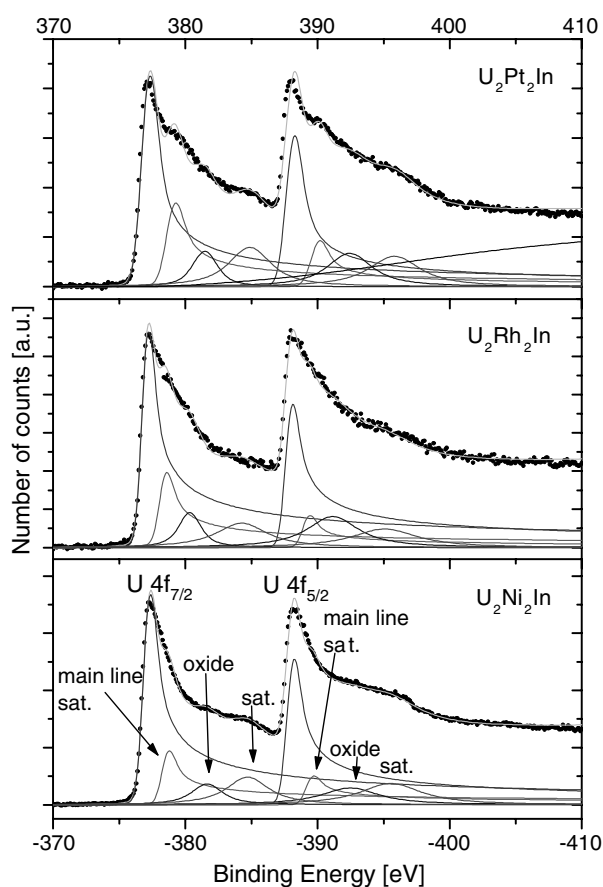


Figure 6. The measured XPS U 4f core-level spectra of U_2T_2In ($T = Ni, Rh, Pt$) and its decomposition into main lines and satellites. The backgrounds are subtracted. Solid circles represent the experimental data. The lines represent the calculated component curves obtained by least square fitting. The interpretation of the individual peaks is given in the text.

Table 3. Peak positions of the main line, spin-orbit splitting the singularity indices α , FWHMs, peak intensities, and the relative intensities of the satellite lines.

Compounds	Peak position (eV)	Δ_{LS} (eV)	α	Satellite peak position (eV)	FWHM (eV)	Int. ^a (%)
U_2Ni_2In	-377.1(1)	10.9	0.41	-384.7(1)	3.54(14)	3.33
U_2Rh_2In	-377.0(1)	10.8	0.45	-384.3(1)	4.40(21)	3.04
U_2Pt_2In	-377.1(1)	10.9	0.34	-384.9(1)	3.40(15)	2.51

^a The column labelled 'Int.' presents the ratio of the integrated intensities of the satellites to those of the main peaks.

The positions of the peaks corresponding to the $U 4d_{5/2}$ and $U 4d_{3/2}$ states are -738.7 and -780.5 eV for U_2T_2In ($T = Ni, Rh$) and -737.6 and -780.0 eV for U_2Pt_2In . All these values are larger than those of pure uranium, i.e., -736.2 and -778.3 eV, respectively [33]. Thus, the shift of the peaks is positive and amounts to $+2.5(2)$ eV for U_2Ni_2In and U_2Rh_2In and $+1.1(2)$ eV for U_2Pt_2In .

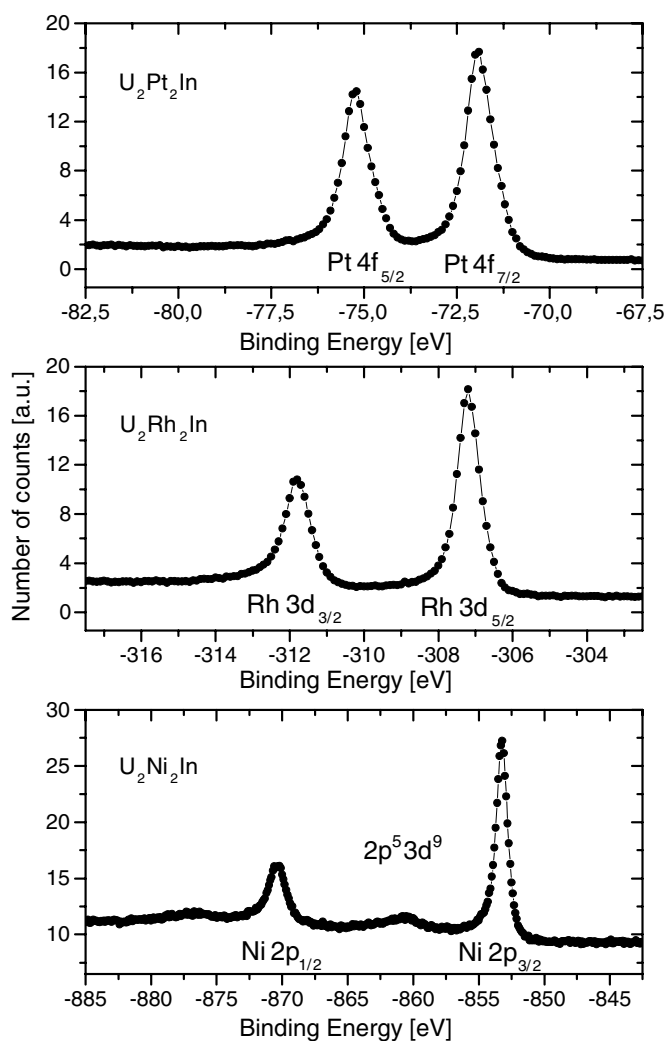


Figure 7. XPS spectra of Ni $2p_{3/2}$ and Ni $2p_{1/2}$ in U_2Ni_2In , Rh $3d_{3/2}$ and Rh $3d_{5/2}$ in U_2Rh_2In and Pt $4f_{7/2}$ and Pt $4f_{5/2}$ in U_2Pt_2In .

4.2.2. nd core level ($n = 3$ (Ni), 4 (Rh) and 5 (Pt)). The Ni $2p$ XPS states have a complex structure (figure 7). The Ni $3p_{3/2}$ and Ni $3p_{1/2}$ bands are located at positions -853.2 and -870.3 eV, respectively. These values are practically the same as the reference value for pure Ni, i.e. -853.0 and -870.5 eV, respectively.

However, the Ni $2p_{3/2}$ peak, located at -853.2 eV below the Fermi level, has two additional satellites situated at -853.8 and -860.7 eV, respectively. These satellites have been observed in Ni metal, $TbNi_2Ge_2$ and Fe_2NiAl [49] and $SmNi_2B$ [50]. Because the intensity of the peak in U_2Ni_2In is smaller than that for the pure Ni metal, one expects the Ni moment to vanish. On the other hand, the existence of these satellites may suggest that the Ni $3d$ band is not completely filled [50, 51]. This is in agreement with the neutron diffraction data for a U_2Ni_2In single crystal which give no evidence for any moment in Ni atoms [13].

The Rh $3d_{5/2}$ and Rh $3d_{3/2}$ lines at U_2Rh_2In are observed at positions -307.2 and -311.8 eV, respectively. These values are identical to those of pure Rh [33].

The Pt $4f_{7/2}$ and Pt $4f_{5/2}$ peaks are located at -71.9 and -74.1 eV, respectively. These values are slightly different from the reference data for pure Pt (-71.2 and -75.1 eV) [32]. The shift for Pt $4f_{7/2}$ states is found to be about $+0.7(2)$ eV.

4.2.3. In core levels. The In $3d_{3/2}$ and In $3d_{5/2}$ peaks for all three compounds are located at -443.35 and -450.8 eV below the Fermi level, respectively. Each peak can be fitted by a single, slightly asymmetric profile. These values are smaller than those for pure In. The shift is found to be $-0.45(2)$ eV. In U_2Rh_2In the In $4d_{5/2}$ and In $4d_{3/2}$ states are at the positions -16.4 and -17.2 eV, which are different than those for the pure In, i.e. -16.6 and -17.4 eV. The shift is again found to be negative, about $-0.2(2)$ eV. In this compound the In $3p_{3/2}$ and In $3p_{1/2}$ states are located at -664.3 and -703.4 eV, respectively, while for pure In the corresponding bands have energies of -665.2 and -703.1 eV, respectively [33].

5. Discussion

In this work we present the XPS spectra collected for the U_2T_2In ($T = Ni, Rh, Pt$) compounds at room temperature and the corresponding density of state calculated in the framework of the scalar-relativistic LMTO and full-relativistic FPLO approach.

The experimental spectra of the valence bands and calculated values of the DOS give similar results (see figure 3). Near the Fermi level the sharp peak corresponding to the U 5f states and the broad maxima connected with the n d bands of the T (Ni, Rh, Pt) elements are observed. A similar valence band is observed for the isostructural U_2Ru_2Sn compounds [47]. In this case the lowest-energy narrow peak results from the U 5f electrons, while at higher binding energies the contributions from the Ru 4d electrons dominate. The calculated DOS indicates that the Fermi energy cuts the peak corresponding to be U 5f states (see figure 3). The peaks of U 5f states in U_2T_2In ($T = Rh, Pt$) are placed below E_F at -0.15 eV whereas for U_2Ni_2In they are at -0.35 eV. The small difference between the position of the U 5f peaks in U_2Ni_2In and the U_2Rh_2In and U_2Pt_2In is probably responsible for the difference in the magnetic properties of these compounds (see section 1).

The results of the calculations indicate that the density of states at the Fermi level is formed mainly by the U 5f but also by the U 5s, T ns and In 5s states. The calculated numbers of states and density of states at the Fermi level obtained by the FPLO method are given in table 4. The Fermi level is located in the U 5f peak; therefore the total DOS (E_F) is dominated by 5f electrons from U atoms. Any small change of the Fermi level causes a large change in the density of states. The calculated values of the density of states at the Fermi level are equal to 53.82 states eV^{-1} for U_2Ni_2In , 31.37 states eV^{-1} for U_2Rh_2In and 63.63 states eV^{-1} for U_2Pt_2In , respectively. The corresponding values of the γ coefficient of the electronic specific heat are equal to 161.85 mJ/mol K^2 for $T = Ni$, 94.35 mJ/mol K^2 for $T = Rh$ and 191.38 mJ/mol K^2 for $T = Pt$, respectively. The experimental values of the γ coefficient of the electronic specific heat are equal 206 mJ/mol K^2 for U_2Ni_2In , 280 mJ/mol K^2 for U_2Rh_2In and 850 mJ/mol K^2 for U_2Pt_2In .

The ratio of the experimental γ_{ex} and calculated γ_{cal} values of the electronic coefficient of the specific heat are equal to 1.28 for U_2Ni_2In , 2.96 for U_2Rh_2In and 4.44 for U_2Pt_2In . The experimental data are strongly enhanced by electron interactions typical for spin fluctuation or heavy fermion systems. In Kondo systems formation of a virtual-bound state causes a significant increase in the density of state and an enhancement of the γ coefficient. Data for the isostructural Kondo system U_2Ru_2Sn gives the value of this ratio equal to 1.4 [47].

Table 4. Numbers of states for U_2T_2In ($T = Ni, Rh, Pt$) compounds per formula unit 2:2:1 and value of the density of states on the Fermi level in the paramagnetic compounds determined from the calculations by the FPLO method.

Atom	Valence electrons				Total
	s	p	d	f	
U_2Ni_2In					
2U	1.098	0.330	4.566	5.562	11.556
2Ni	1.502	1.358	17.534	0.000	20.394
In	1.322	1.720	9.96	0.000	13.002
Total (per f.u.)	3.922	3.408	32.060	2.781	44.952
$N(E_F) = 53.82 \text{ states eV}^{-1}$					
U_2Rh_2In					
2U	0.752	0.322	4.66	5.656	11.388
2Rh	1.286	1.470	15.954	0.000	18.716
In	1.247	1.592	9.963	0.000	12.802
Total (per f.u.)	3.285	3.390	30.577	5.656	42.906
$N(E_F) = 31.37 \text{ states eV}^{-1}$					
U_2Pt_2In					
2U	0.926	0.464	4.294	5.642	11.326
2Pt	1.922	1.694	17.08	0.000	20.696
In	1.316	1.654	9.973	0.000	12.943
Total (per f.u.)	4.164	3.813	31.347	5.642	44.965
$N(E_F) = 63.63 \text{ states eV}^{-1}$					

In the next step, the hybridization between the U 5f uranium atoms and n d electrons of the T element are analysed. The U 5f states form the peaks at the Fermi level and above. Below the Fermi level (in the region 0 to -5 eV for U_2Ni_2In and U_2Rh_2In and 0 to -6.5 eV for U_2Pt_2In) a broad peak with a small intensity, connected with the U 6d states, is observed. The nd states are in the -1.5 to -4.2 eV for Ni 3d states in U_2Ni_2In , -1.1 to -5 eV Rh 4d states and -2.5 to -6.5 eV for Pt 5d states in U_2Pt_2In . A shift of the position of the peak corresponding to the nd states from the Fermi level is observed in the calculated DOS for the U_2T_2In series of compounds (see figure 3 in [5]). This tendency is not correlated with the magnetic properties of these compounds. U_2Co_2In is a weak paramagnet, U_2Ni_2In an antiferromagnet, U_2Rh_2In a spin fluctuator, U_2Pd_2In an antiferromagnet and U_2Pt_2In a spin fluctuator [3–6]. The change in DOS is connected with the increase in the electronic coefficient of the specific heat which increases from 32 mJ/mol K^2 for U_2Co_2In to 850 mJ/mol K^2 for U_2Pt_2In [6].

The above data suggest hybridization between the nd electrons of the T element and U 6d electrons of the uranium atoms. Probably appreciable charge transfer occurs between d- and f-states of U atoms and d-states of the transition metal, leading to nearly filled d-states of the T element. This mechanism leads to non-integer 5f occupancy and automatically to a reduction of the uranium magnetic moment.

The analysis of U $4f_J$ ($J = 7/2$ and $5/2$) lines and the satellite associated with these lines indicates that the main line is shifted asymmetrically and the intensity of a broad ~ 7 eV satellite is larger for more localized 5f electron systems, i.e. for the case with weak f–ligand hybridization. For the compounds exhibiting Pauli paramagnetism the satellites have

lower intensities and the satellite width should be wider than that for magnetically ordered samples [40].

The results for the investigated compounds (see table 4) indicate that the singularity indices α for U_2Ni_2In and U_2Pt_2In are smaller than those for U_2Rh_2In . This result also seems to correlate with the magnetic properties of these compounds. The first two compounds show a more localized character of the 5f electrons. This feature reflects the intensities of the satellite peaks which are relatively low in U_2Rh_2In . The origin of the first satellite, which is located about 3.1 eV higher than the main line, is not clear. It seems that the occurrence of this satellite is characteristic for some U-based ternary intermetallics. According to Fujimori *et al* [52], the presence of the symmetric peak at 7.0 eV (the $5f^2$ final state) below the main line gives evidence that the uranium atoms in these compounds are partially localized and partial itinerant.

On the basis of the calculations of the density of states one expects that there is the hybridization (see figure 4) between U 6d and T *nd* electrons. The experimental data obtained for a large number of U_2T_2X ($X = Sn, In$) compounds point out that such hybridization of the 5f states of the uranium atoms and the d-states of the transition metal, for example $T = Ni, Rh, Pt$ atoms, is possible. In order to verify this the interatomic distances between U–U, U–T and U–In atoms are analysed based on the formalism proposed by the Harrison–Stroub model [53–55]. The calculated covalent energy indicates that the magnetism of the U_2T_2In ($T = Ni, Rh$) compounds is governed by the f–d hybridization because the hybridization matrix element V_{fd} is larger and the values of V_{ff} and V_{fp} are considerably smaller. According to references [3, 10], the hybridization of the 5f electrons of uranium with the 4d electrons of rhodium in U_2Rh_2In and the 5d electrons of platinum in U_2Pt_2In is much stronger than those between the 5f states of uranium and the 3d states of nickel in U_2Ni_2In . Comparing the calculated hybridization energy with the Doniach model [56], one obtains that U_2Pt_2In compounds are located near the magnetic–nonmagnetic border in the Doniach diagram (see figure 3 in [10]) while U_2Ni_2In is in the magnetic and U_2Rh_2In in nonmagnetic region [10]. A similar conclusion was drawn by Diviš *et al* [23, 24], who have also performed band structure calculations. The calculated value of the charge transfer in the isostructural U_2Ni_2Sn compound suggests that the U–Ni interaction should be weaker [24]. This compound is an antiferromagnet like U_2Ni_2In , with Néel temperature equal to 25 K [6].

The Ni ($2p_{1/2}$) and Ni ($2p_{3/2}$) satellite peaks observed for U_2Ni_2In suggest that the Ni 3d band is not completely filled. However, the question arises, whether the Ni atoms do carry a small magnetic moment. Neutron powder diffraction experiments [8, 9] do not give a clear answer, since a magnetic moment of $\sim 0.4 \mu_B$ at the Ni site was reported [8]. Nevertheless, this result has not been confirmed by neutron diffraction data [13] carried out on single crystals, which indicate the absence of the magnetic moments on the uranium atoms [13].

The analysis of the core levels of various elements gives information about the chemical shift which originates from changes of the potential related to the formation of compounds. As a result, the binding energies of electronic levels are different in compounds and in pure elements. The results presented in this work indicate that the lines corresponding to the uranium core levels do not change. For the T element, a positive shift is observed for $T = Ni$ and Pt, while for $T = Rh$ the core levels do not change. The In lines have negative shift. The negative shift may be related to some charge transfer towards these atoms.

6. Conclusions

The XPS study at room temperature combined with calculations of the density of states for U_2T_2In ($T = Ni, Rh, Pt$) reveal information on the electronic structure of these compounds. The agreement between the measured XPS spectra and the calculated ones is reasonably good.

The calculations of the density of states using the TB-LMTO and FPLO methods can be summarized by four distinct features.

- (1) The density of states of width of an order of 1 eV derived from the U 5f-electrons lies essentially above the Fermi level at -0.35 eV for U_2Ni_2In and -0.15 eV for U_2Rh_2In and U_2Pt_2In ,
- (2) Below the U 5f peaks, broad peaks at -2.0 eV for Ni 3d in U_2Ni_2In , at -2.7 eV for Rh 4d in U_2Rh_2In and at -4.0 eV for Pt 5d in U_2Pt_2In are observed. The widths of these peaks are found to amount to 2.1 eV in U_2Ni_2In , 2.6 eV for U_2Rh_2In and 3.3 eV in U_2Pt_2In .
- (3) The contribution of the 5s- and 5p-states of the indium atoms to the density of states is minor.
- (4) The general features of the density of states of U_2T_2In ($T = Ni, Rh, Pd$) calculated by the LMTO method in this work agree reasonably with previous investigations [23–25]. Data from the full-relativistic spin-orbit FPLO method give the realistic spin-orbit splitting of the U 5f-states. Our calculated and experimental data for U_2Pt_2In do not give the wide break between Pt 5d states and U 5f states suggested from the calculations using the HLCO method [6].

The main XPS experimental results can be outlined as follows.

- (1) The valence band is formed from an overlap of the U(5f) and Ni(3d), Rh(4d) and Pt(5d) bands. The narrow band of the 5f-electrons lies essentially below the Fermi level, whereas the T *nd* electrons form a broad band. Very small differences in the position of the U 5f peak are observed. The peaks corresponding to the *nd* states of the transition elements widen and shift the peaks to lower energies in the series $T = Ni, Rh$ and Pt , which is in good agreement with the calculated data.
- (2) Analysis of the U 4f core-level spectrum based on its decomposition into main lines and satellites and taking into account the relations of the satellite intensity and singularity index to the width of the satellite leads to the conclusion that the ground state of U_2Ni_2In is magnetic, but that of U_2Rh_2In is nonmagnetic. The situation for U_2Pt_2In is not clear due to its complex crystal structure.

Acknowledgments

The work of AJ was partially supported by the Centre of Excellence for Magnetic and Molecular Materials for the Future Electronics within the European Commission Contract No G5MA-CT-04049.

References

- [1] Peron M N *et al* 1993 *J. Alloys Compounds* **201** 203
- [2] Mirambet F, Gravereau P, Chevalier B, Trut L and Etourneau J 1993 *J. Alloys Compounds* **191** L1
- [3] Nakotte H 1994 *PhD Thesis* Universited of Amsterdam, Amsterdam, p 101 and references therein
- [4] Prokeš K 1997 *Thesis* Universite of Amsterdam, Amsterdam, p 163 and references therein
- [5] Havela L *et al* 1994 *J. Appl. Phys.* **76** 6214
- [6] Havela L *et al* 1995 *J. Magn. Magn. Mater.* **140–144** 1367
- [7] Bourée F, Chevalier B, Fournés L, Mirambet F, Roisnel T, Tran V H and Żołnieriek Z 1994 *J. Magn. Magn. Mater.* **138** 307
- [8] Nakotte H *et al* 1996 *Phys. Rev. B* **53** 3263
- [9] Tran V H, Żołnieriek Z, Bourée F and Roisnel T 1996 *J. Magn. Magn. Mater.* **161** 270
- [10] Tran V H, Żołnieriek Z, Zaleski A J and Noël H 1997 *Solid State Commun.* **101** 709
- [11] du Plessis P de V, Strydom A M and Tran V H 1999 *Solid State Commun.* **112** 391

- [12] Tran V H, Hoser A and Hofmann M 2000 *J. Phys.: Condens. Matter* **12** 1029
- [13] Martin-Martin A, Pereira L C J, Lander G H, Rebizant J, Wastin F, Spirlet J C, Dervengas P and Brown P 2000 *Phys. Rev. B* **59** 11818
- [14] Richter M, Zahn P, Diviš M and Merting I 1996 *Phys. Rev. B* **54** 11985
- [15] Prokeš K, Nakotte H, Bartashevich M I, Doerr M and Sechovsky V 2003 *Phys. Rev. B* **68** 014405
- [16] Kim J S, Alwood J, Getty S A, Sharifi F and Stewart G R 2000 *Phys. Rev. B* **62** 6986
- [17] Tran V H, Paschen S, Rabis A, Baenitz M, Steglich F, du Plessis P de V and Strydom A M 2003 *Phys. Rev. B* **67** 075111
- [18] Estrela P, Pereira L C J, de Visser A, de Boer F R, Almeida M, Godinho M, Rebizant J and Spirlet J C 1998 *J. Phys.: Condens. Matter* **10** 9465
- [19] Hill H H 1970 *Photonium 1970 and Other Actinides* ed W N Miner (New York: Metallurgical Society of the AIME) p 2
- [20] Andersen O K and Jepsen O 1984 *Phys. Rev. Lett.* **53** 2572
- [21] Koepernik K, Velicky B, Hayn R and Eschrig H 1997 *Phys. Rev. B* **55** 5717
- [22] Koepernik K and Eschrig H 1999 *Phys. Rev. B* **59** 1743
- [23] Diviš M, Richter M and Eschrig H 1994 *Solid State Commun.* **90** 99
- [24] Diviš M, Olšovec M, Richter M and Eschrig H 1995 *J. Magn. Magn. Mater.* **140–144** 1365
- [25] Matar F S 1995 *J. Magn. Magn. Mater.* **151** 263
- [26] Suzuki S et al 1993 *Japan. J. Appl. Phys.* **8** 59
- [27] Ejima T et al 1994 *J. Phys. Soc. Japan* **63** 2428
- [28] von Barth U and Hedin L 1972 *J. Phys. C: Solid State Phys.* **5** 391
- [29] Hu D and Langreth D C 1985 *Phys. Scr.* **32** 391
- [30] <http://www.FPLO.de>
- [31] Perdew J P and Wang Y 1992 *Phys. Rev. B* **45** 13244
- [32] Yeh J J and Lindau I 1985 *At. Data Nucl. Data Tables* **32** 1
- [33] Hufner S 1994 *Photoelectron Spectroscopy* (Berlin: Springer) p 453
- [34] Ogasawara H, Kotani A and Thole B T 1994 *Phys. Rev. B* **50** 123
- [35] Thole B T, Wang X D, Harmon B N, Li D and Dowben P A 1993 *Phys. Rev. B* **47** 90
- [36] Talik E, Neumann M and Mydlarz T 1998 *J. Magn. Magn. Mater.* **189** 183
- [37] Sato N K, Aso N, Miyake K, Shiina R, Thalmeier P, Varelogiannis G, Geibel C, Steglich F, Fulde P and Komatsubara T 2001 *Nature* **410** 340
- [38] Zwicknagl G, Yaresko A and Fulde P 2002 *Phys. Rev. B* **65** 081103(R)
- [39] Zwicknagl G, Yaresko A and Fulde P 2003 *Phys. Rev. B* **68** 052508
- [40] van Veenendaal M A, Eskes H and Sawatzky G A 1993 *Phys. Rev. B* **47** 11462
- [41] Bocquet A E, Mizohawa T, Fujimori A, Matoba M and Anzani S 1995 *Phys. Rev. B* **52** 13838
- [42] Doniach S and Sunjić M 1970 *J. Phys. C: Solid State Phys.* **3** 285
- [43] Tougaard S 1990 *J. Electron Spectrosc. Relat. Phenom.* **52** 243
- [44] Talik E, Lucas M E, Suski W and Troć R 2003 *J. Alloys Compounds* **350** 72
- [45] Ejima T, Sato S, Suzuki S, Saito Y, Fujimori S, Sato N, Komatsubara M and Kasuya T 1996 *Phys. Rev. B* **53** 1806
- [46] Chelkowska G, Morkowski J A, Szajek A and Troć R 1992 *J. Phys.: Condens. Matter* **14** 3199
- [47] Chelkowska G, Morkowski J A, Szajek A, Stępień-Damm J and Troć R 2003 *Eur. Phys. J. B* **35** 349
- [48] Ejima T, Sato S, Saito V, Fujimori S, Sato N, Komatsubara T, Kasuya T, Oniaki Y and Ishii T 1996 *Phys. Rev. B* **53** 1806
- [49] Guzik A, Talik E and Kuznietz M 2004 *J. Magn. Magn. Mater.* **272–276** e589
- [50] Hong N M, Thuy N P, Schandy G, Holubar T, Hilscher G and Franse J J M 1993 *J. Appl. Phys.* **73** 5698
- [51] Toliński T, Chelkowska G and Kowalczyk A 2002 *Solid State Commun.* **122** 145
- [52] Fujimori S, Saito Y, Sato N, Komatsubara T, Suzuki S, Sato S and Ishii T 1998 *Solid State Commun.* **105** 185
- [53] Harrison W A 1983 *Phys. Rev. B* **28** 550
- [54] Straub G K and Harrison W A 1985 *Phys. Rev. B* **31** 7668
- [55] Harrison W A and Straub G K 1987 *Phys. Rev. B* **36** 2695
- [56] Doniach S 1977 *Physica B* **91** 231